Nanomechanical Characterization of the Stiffness of Eye Lens Cells: A Pilot Study

Amela Hozic, Felix Rico, Adai Colom, Nikolay Buzhynskyy, Simon Scheuring

Nanomechanical Characterization of the Stiffness of Eye Lens Cells: A Pilot Study

Amela Hozic,[1,3] *Felix Rico,*[2,3] *Adai Colom,*[2] *Nikolay Buzhynskyy,*[2] *and Simon Scheuring*[2]

Purpose. The purpose of this study is to probe the mechanical properties of individual eye lens cells isolated from nucleus and cortex of adult sheep eye lens, and to characterize the effect of cytoskeletal drugs.

Methods. We used atomic force microscopy (AFM), featuring a spherical tip at the end of a soft cantilever, to indent single lens cells, and measure the Young's modulus of isolated nuclear and cortical lens cells. Measurements were performed under basal conditions, and after addition of drugs that disrupt actin filaments and microtubules.

Results. We found that single lens cells were able to maintain their shape and mechanical properties after being isolated from the lens tissue. The median Young's modulus value for nuclear lens cells (4.83 kPa) was ~ 20-fold higher than for cortical lens cells (0.22 kPa). Surprisingly, disruption of actin filaments and microtubules did not affect the measured Young's moduli.

Conclusions. We found that single cells from the lens nucleus and cortex can be distinguished unambiguously using the elastic modulus as a criterion. The uncommon maintenance of shape and elastic properties after cell isolation together with the null effect of actin filaments and microtubules targeting drugs suggest that the mechanical stability of fiber cells is provided by cellular elements other than the usual cytoskeletal proteins. (*Invest Ophthalmol Vis Sci.* 2012;53:2151–2156) DOI:10.1167/iovs.11-8676

The eye's lens is a biological marvel. It is the only transparent tissue in our body. Transparency is assured by lens architecture and its unusual developmental program. The lens is an avascular tissue of complex structure that comprises about 1000 layers of perfectly clear fiber cells packed tightly to enable light to pass across cell boundaries without scattering.[1,2] During development, the fiber cells initiate a degradation process of nucleus and organelles that would obstruct the light path.[3] What remains is the cytoplasm consisting of an unusually thick solution of special proteins, called crystallins, which are highly ordered to provide a high refractive index.[4]

The organization of the lens resembles an onion, in which each layer of cells is at a different stage of lens cell differentiation and maturation. The undifferentiated cells comprise the outermost layer at the anterior of the lens. Newly differentiated and young fiber cells are in subsequent layers (cortical fiber cells), and the oldest fiber cells are in the central layers (nuclear fiber cells).[5] The lens nucleus is compact. Cortical cells are packed less densely, and reveal less rigidity as a sub-tissue. The lens focuses light onto the retina, where photoreception takes place. To focus to different distances, the lens must adapt its shape. This adjustment, known as accommodation, implies that the lens is, in contrast to a solid glass lens, flexible.[6]

The loss of lens elasticity is thought to be one of the primary causes for the best-known age-related vision changes: decrease in the sharpness of vision and loss of focusing power of the lens.[7] It has been shown that stiffness of the center and periphery of lens tissue increases with aging.[8–10] This is most pronounced in the nucleus – the stiffness of the lens center was found to increase by approximately 1000 times and the outer region of the lens by a factor of 50.[8] While in these previous studies researchers were focused on the lens tissue in general, it is of interest to look at the individual cell level, as growing number of studies demonstrate a close association between cell mechanical properties and various disease conditions.[11]

Atomic force microscopy (AFM)[12] is a powerful technique for biological sciences, as it allows samples to be studied directly under physiological conditions, such as in physiological buffer, under ambient pressure and temperature. During recent years, AFM has been applied to studying the mechanical properties (such as stiffness, viscoelasticity, and adhesion) of various biological samples.[13–16] The pioneering work of Radmacher et al. showed the capacity of AFM to measure quantitatively the elastic properties of cells as a function of the position of the AFM tip on the cell.[17] The technique's sensitivity has been used extensively over the last several years to distinguish normal and pathological phenotypes of various cell types by their differing mechanical properties.[18–23]

AFM combined with optical microscopy allows positioning of the AFM tip onto a cell or even onto a particular region of a cell, as well as monitoring the integrity and morphology of the cell during the investigation by AFM.[24] Although some recently published reports used AFM to study the mechanics of ophthalmic tissues,[25,26] AFM still is used rarely in vision science, suggesting its unrealized potential in this field.[27]

We describe the use of AFM to study lens cell stiffness. We measured elastic properties of individual nuclear and cortical lens cells. Quantitative characterization of each type of lens cells was performed by the determination of the elasticity, the

From the [1]Division for Marine and Environmental Research, Ruder Boskovic Institute, Zagreb, Croatia, and [2]U1006 INSERM, Aix-Marseille Université, Parc Scientifique et Technologique de Luminy, Marseille, France.

[3]These authors equally contributed to the work.

Supported by the Agence Nationale de la Recherche (ANR), and the 'City of Paris' (to SS) and a European Community Marie Curie Intra-European Fellowship for Career Development (to FR), and by the Croatian Ministry of Science, Education and Sports, project No. 0982934–2744 (AH).

Submitted for publication September 27, 2011; revised January 29, 2012; accepted March 7, 2012.

Disclosure: **A. Hozic**, None; **F. Rico**, None; **A. Colom**, None; **N. Buzhynskyy**, None; **S. Scheuring**, None

Corresponding author: Simon Scheuring, U1006 INSERM, Aix-Marseille Université, Parc Scientifique et Technologique de Luminy, 163 avenue de Luminy, 13009 Marseille, France; simon.scheuring@inserm.fr; Telephone ++33 (0)4 91 82 87 77; Fax ++ 33 (0)4 91 82 87 01.

Young's modulus. The obtained Young's modulus for nuclear cells was found to be ~ 20 times higher than for cortical cells, showing that the cortical cells are significantly more compliant and, thus, deformable. The technique presented is sufficiently sensitive to distinguish nuclear from cortical cells unambiguously, and will open a novel avenue for the quantitative study of lens cell aging and pathology.

METHODS

Preparation of Cells

Three lenses from healthy sheep 5 ± 2 years old were obtained from INRA (Institut National de la Recherche Agronomique) UCEA (Unité Commune d'Expérimentation Animale, Jouy-En-Josas, France). Enucleation occurred within 1 hour of death, with lenses frozen immediately after removal from the eye by dropping them in liquid nitrogen and subsequently stored at −80°C until used. All animal treatment has been conducted respecting the current European and French rules (https://www.jouy.inra.fr/ucea/en_savoir_plus/ethique_et_reglementation) and the ARVO Statement for the use of Animals in Ophthalmic and Vision Research.

Prior to AFM measurements, the lenses were thawed in buffer A (10 mM Tris pH 8.0; 5 mM EGTA; 5 mM EDTA). The equatorial diameter of lenses was ~ 15 mm. The transparency of the lenses and absence of cataracts was verified before dissection. Eye lenses were dissected in 2 mL (per lens) of buffer A. The method of isolation of fiber cells was similar to that described by Garland et al.[28] in that different layers of cells were stored separately. After careful capsule removal using tweezers, cortical cells were separated gently from the nucleus by flushing buffer over the lens tissue using a 1 mL pipette. The pipette flow was enough to separate the outermost (2 mm) cortical cells. After separation, the cortical cells were put in a 15 mL Falcon tube with buffer A solution and placed on the Vari-Mix variable speed test tube rocker on low speed for 30 minutes to allow uniform suspension of cortical cells. The remaining lens fraction was flushed continuously with the pipette until only the innermost 5 mm of the lens was left. This innermost nucleus then was placed on the Vari-Mix to obtain a uniform suspension that we considered to be composed of nuclear cells only. Although relatively slow, this method assured gentle separation of cortical and nuclear cells.

For cell immobilization, glass bottom Petri dishes (50 mm diameter) were pretreated using 0.1% poly-l-lysine (Sigma Aldrich, St. Louis, MO). 1 mL of poly-l-lysine solution was incubated on the glass surface for 1 hour. The glass bottom Petri dishes then were rinsed with PBS (3 × 2 mL) and 2 mL of cell suspension were pipetted onto the immersed poly-l-lysine coated glass surface. After 2 hours of incubation time, cell attachment was checked using optical microscopy. To remove loosely attached cells, the Petri dish was rinsed softly 10 times with PBS.

Cytoskeletal Disruption Experiments

To measure the influence of cytoskeletal components on the elasticity of lens cells, both types of lens cells, cortical and nuclear, were treated with cytochalasin B (Sigma Aldrich) and nocodazole (Sigma Aldrich) for 1 hour before force measurements. Cytochalasin B and nocodazole were dissolved in dimethylsulfoxide (DMSO). The final concentrations of the drugs used in cell samples were 10 μM for cytochalasin B and 16 μM for nocodazole. The Petri dishes contained 2 mL of PBS with lens cells. To circumvent diffusion-limited drug delivery to the cells, we exchanged half of the volume of the medium with half of the volume that contained the drug, and then aspirated and ejected half of the medium back and forth into and out of the pipette and the Petri dish, respectively.

Atomic Force Microscopy

A BioScope Catalyst (Bruker, Santa Barbara, CA) mounted on an inverted optical microscope (X71 Olympus, Tokyo, Japan) was used in force mode for mechanical measurements. The glass bottom Petri dish was mounted in a sample holder, which was fixed by magnets to the base of the AFM. All force measurements were performed in PBS buffer at room temperature. The entire microscope was placed on a vibration isolation table.

Force measurements were performed using a spherical SiO_2 tip of 1 μm diameter attached at the end of a silicon nitride cantilever with a nominal spring constant of 0.06 N/m (Novascan Technologies Inc., Ames, IA). The precise value of the spring constant of the cantilever was determined by the thermal fluctuation method after calibration of the deflection sensitivity.[29]

For topography imaging and mechanical mapping of lens cells we used PeakForce Tapping mode.[30,31] PeakForce Tapping was performed using silicon nitride AFM cantilevers with pyramidal tips (ScanAssist-Fluid, Bruker, nominal resonance frequency in air 150 kHz, nominal spring constant 0.7 N/m). The scanning rate was set to 0.5 Hz at 256 samples per line and a force set point of 250 pN.

Force Curves

In force-distance (*F-z*) curves, the deflection of the cantilever is measured as the AFM tip approaches and retracts from the sample surface. Typically, the deflection is plotted against the vertical position of the piezo (*z*-position). The cantilever deflection (d) is translated into force (F) following Hooke's law, $F = kd$, where k is the spring constant of the cantilever. On stiff samples ($k_{(object)} \gg k_{(cantilever)}$), the deflection of the cantilever is directly proportional to the vertical travel of the piezo once the AFM tip has touched the surface. On soft samples, the *z*-piezo movement will result in cantilever bending and the indentation of the sample.[32] By using a spherical tip the force-distance curve can be fitted using the Hertzian model to derive the elastic properties, that is the Young's modulus, of the sample.

Data Analysis

The Young's modulus (E) was estimated assuming Hertzian contact of a sphere indenting an elastic half-space.[33,34] The Hertz model was fitted to approaching force-distance curves

$$F = \frac{4}{3}\frac{E}{1-\nu^2}\sqrt{R}\delta^{3/2} \quad (1)$$

where ν is the Poisson ratio (assumed to be 0.5), R is the radius of the spherical bead, and δ is the indentation, calculated in terms of the point of contact (z_c) and the deflection offset (d_0) as $\delta = z - z_c - (d - d_0)$.

Statistics

The mean of the Young's modulus values obtained on different regions on a cell was used as representative of cellular elasticity. Difference in E obtained on nuclear and cortical cells was analyzed using the Wilcoxon rank sum test for equal medians. Statistical significance was assumed at $P < 0.05$.

RESULTS

We used an AFM featuring a flexible soft cantilever with a spherical tip at its end to probe the elasticity of cortical and nuclear lens fiber cells (Fig. 1A). Combination of AFM with optical microscopy enabled precise positioning of the AFM tip to perform force spectroscopy on cells and subregions of cells of interest. A bright field image of the cantilever, where the spherical tip is attached, and lens cells that are immobilized firmly to the glass surface allowed efficient probing of lens cell elasticity (Fig. 1B). A representative force-distance curve fitted using equation 1 to derive the mechanical properties (Young's modulus) of the sample is shown in Figure 1C.

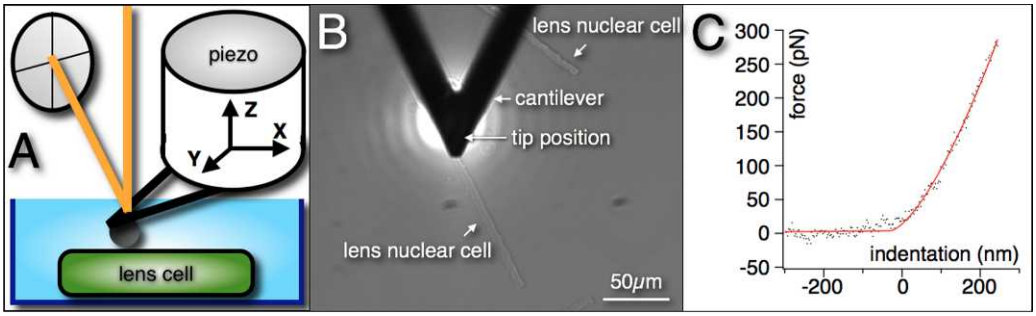

Figure 1. Experimental setup and rationale. (**A**) Schematic drawing of the experimental setup. A spherical tip (diameter: 1 μm) mounted on a cantilever (nominal spring constant 0.06 N/m) was indented into lens cells immersed in PBS. The tip movement was mediated using a piezoelectric stage, while the deflection (force) exerted on the cantilever was monitored on a split photodiode via a reflected laser beam (orange line). (**B**) The AFM setup was coupled to an inverted optical microscope allowing the placement and observation of the cantilever position and the lens cells. The lens nuclear cells appeared as elongated structures with a length of up to more than 100 μm and a width of about 5 μm. (**C**) Representative force-indentation curve and Hertzian fit (red line). The indentation slope following sample contact (0 nm position) reported about the mechanical properties of the cell.

We took special care in isolating lens fiber cells from the cortical and nuclear regions. Our separation method allowed us to obtain individual cells preserving the shape and dimensions found on native lens tissue.[35] From optical images (Fig. 1B), the average ($\pm$ SD) width and length of isolated cells were, respectively, 5.9 $\pm$ 1.4 μm and 129 $\pm$ 137 μm for nuclear cells, and 7.5 $\pm$ 1.6 μm and 61 $\pm$ 24 μm for cortical cells. Cells' thickness was estimated from AFM topographical images and was of $\sim$ 4 μm nuclear and $\sim$ 2 μm for cortical fiber cells (Figs. 2 and 3).

A recently developed imaging mode, PeakForce, enabled concomitant measurement of topography and nano-mechanical properties of the sample, such as elastic modulus and deformation.[31] In this mode, the tip is oscillated at 1 kHz to acquire short range force-distance curves while the sample is scanned in the horizontal plane. The vertical distance, at which the force setpoint is reached, provides information about the topography of the sample, while the slope of the contact region provides estimations of mechanical properties, including deformation and elastic modulus, of lens cortical (Fig. 2) and nuclear (Fig. 3) cells. The cells' thickness (3–6 μm, Figs. 2A and 3A) appeared uniform for both cell types (Figs. 2B and 3B). The maximum deformation of the sample at the peak force is readily an indirect evidence for their difference in cell elasticity (Figs. 2C and 3C). Cortical cells were found more deformable (221 $\pm$ 33.4 nm) than nuclear cells (45.0 $\pm$ 11.3 nm). This is supported further by the elastic modulus maps (Figs. 2D and 3D), which show softer cortical cells compared to nuclear ones. While PeakForce imaging allows the direct structure-nano-mechanics assessment of a sample, due to the sharp pyramidal tip used and the shortness of the force-distance curves acquired, for real quantitative assessment of the mechanical properties of lens cells force-distance curves using spherical tips are preferred. Nevertheless, using PeakForce measurements, the elastic modulus for nuclear cells (Fig. 3D) appeared more than an order of magnitude higher than the values for cortical cells (Fig. 2D). Although qualitative, stiffness maps also allowed us to determine the degree of heterogeneity of large cell areas with a resolution of $\sim$ 100 nm. As can be observed, stiffness maps showed relatively low heterogeneity,

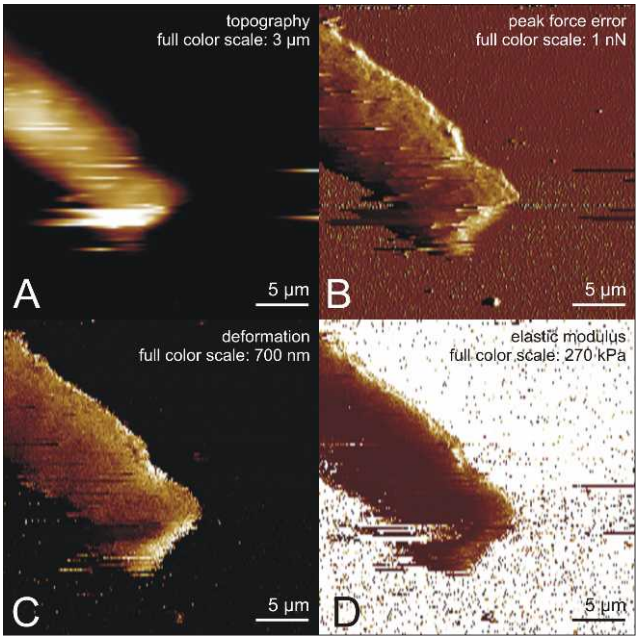

Figure 2. Peak-Force quantitative nano-mechanical (PF-QNM) measurements on a lens cortical cell**.** At each pixel of the image, a force-distance curve was acquired from which the different parameters were extracted. Topography (**A**), peak force error signal (**B**) deformation map (**C**), and elasticity map (**D**) were measured concomitantly. The bright area in **D** corresponds to the hard glass substrate resulting in saturation in the stiffness signal.

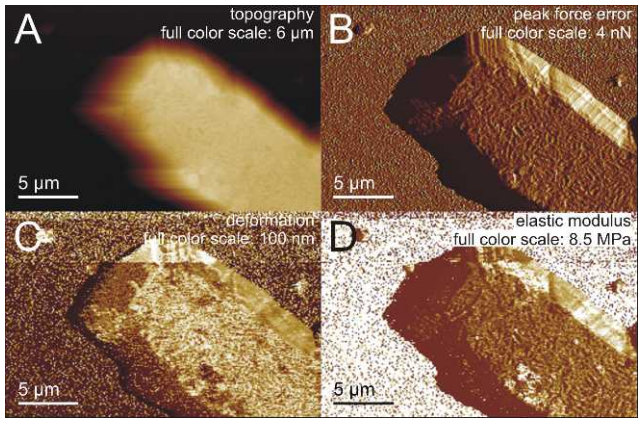

Figure 3. PF-QNM measurements on a lens nuclear cell**.** Topography (**A**), peak force error signal (**B**), deformation map (**C**), and elasticity map (**D**) measured concomitantly. Please note the fine surface structure visible in **A** and **B**.

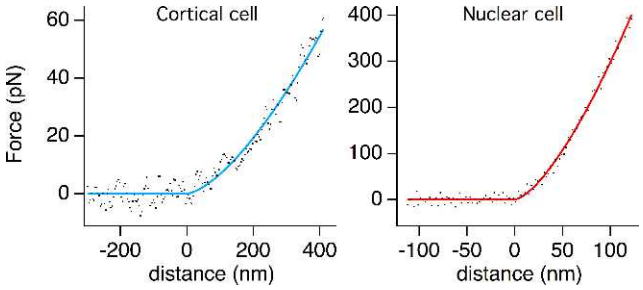

FIGURE 4. Force indentation curves (*F-z*) on cortical and nuclear lens cells. Representative AFM cantilever deflection versus indentation curves on cortical (left) and nuclear (right) cells (black dots). The Young's modulus was determined using the Hertzian contact elastic model (colored lines showed best fits of equation 1). Shown here are the curves of a lens cortical cell with a stiffness of 0.2 kPa (blue, left) and of a lens nuclear cell with a stiffness of 5.4 kPa (red, right). Only approaching curves are shown.

suggesting that measurements obtained at few cell regions provided a reliable estimate of the overall cell elastic response. Representative force-distance curves of cortical and nuclear cells (Fig. 4) varied in slope after the contact point clearly showing the difference in mechanical properties of two cell types (notice the different scales). The nuclear cell was stiffer and less deformable, which caused the cantilever to deflect more giving rise to a steeper slope.

Force measurements were performed on at least 5 randomly chosen regions on 9 cortical and 11 nuclear lens cells. Measurements were not performed on the cell edges to avoid possible substrate contribution. Three force curves were obtained on each region (obtaining a total of 120 and 150 curves, for the cortical and the nuclear cells, respectively). Elastic modulus values obtained from the measurements on cortical cells ranged from 0.094 to 1.02 kPa, while the range for nuclear cells spanned from 1.27 to 11.6 kPa. The derived histogram of the distribution of Young's moduli obtained from the force measurements depicts two clearly separated distributions corresponding to the two cell types (Fig. 5). The lens nuclear cells were an order of magnitude stiffer (median 4.83 kPa, interquartile range [IQR] 3.08–9.27 kPa) than cortical cells (median 0.216 kPa, IQR 0.157-0.388 kPa, $P < 0.001$). Importantly, the results show that probing the mechanical response of 5 regions on an individual cell was sufficient to assign unambiguously the cell type, that is the state of a cell in eye lens development.

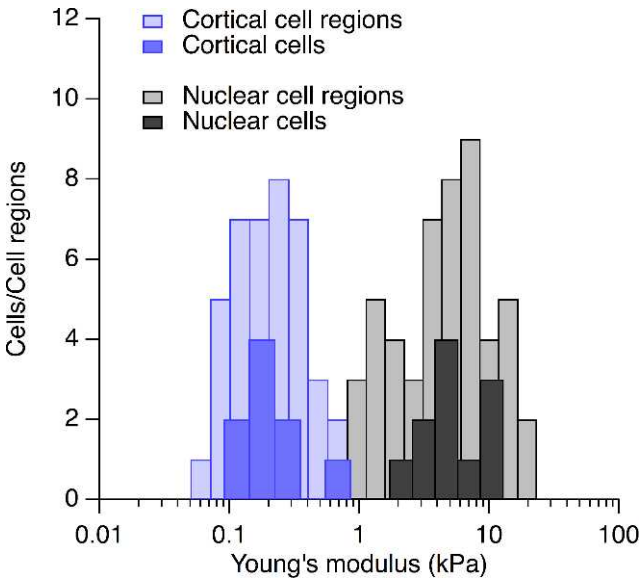

FIGURE 5. Young's moduli derived from the force data collected over 40 regions of 9 cortical lens cells and 50 regions of 11 nuclear lens cells. Light-colored bars show the distribution of values obtained on all different cell regions, while dark-colored bars represent the distribution from different cells. Notice the logarithmic horizontal axis.

Effects of Cytoskeletal Drugs

The effect of cytoskeletal drug action on cell elasticity was investigated by recording force-distance curves on the cells before and after the addition of the drugs. We used cytochalasin B, which is known to disrupt actin filaments, and nocodazole, which disrupts microtubules, aiming at the detection of cytoskeletal elements that may influence the mechanics of lens cells. The results are presented in Table 1. At common working concentrations of 10 μM for cytochalasin B and 16 μM for nocodazole, we measured no significant effect on the mechanical properties of both types of lens cells.

DISCUSSION

This pilot study was done to show that AFM can be used reliably to measure the mechanical properties of the isolated eye lens cells. The values obtained for Young's moduli of sheep lens cells were corroborated when compared to elastic modulus values of other cell types measured by AFM. A recently presented review on cell elasticity summarized Young's moduli of different cell types showing variations of elastic modulus values of living mammalian cells in the wide kPa range (0.1–400 kPa).[36] Moreover, our gentle cell isolation method assured relatively intact cells as verified from their width, length and thickness using optical and AFM images. Previous works measuring the dimensions of cells from the eye lens of sheep and other species are in excellent agreement with our values of width and thickness of nuclear and cortical fiber cells.[35,37]

Data on biophysical and biochemical properties, such as hardness, elasticity, protein content and refractive index distributions of lenses, have been obtained from in vitro studies, and animal lenses are used frequently for this purpose because of their ready availability.[38] In this study, we used sheep lenses because the comparable size and biconvex shape closely resemble that of human, and the biochemistry and membrane architecture have been characterized previously at molecular resolution.[39] From the stiffness of the lens and the anatomy of its structure, it would be expected that the ovine lens is capable of accommodation.[40] On the other hand, it has been shown that the growth rate of primates lenses is different from that of other mammals.[38] Thus, it is expected that the relative stiffness between cortical and nuclear cells may vary importantly among species.

In an attempt to quantify the stiffness of human lens regions, several groups used different techniques on either the

TABLE 1. Effect of Cytoskeletal Drugs on Cell Elasticity

Cell Condition	E_C (kPa)	E_N (kPa)
Untreated cells	0.172 ± 0.087	8.25 ± 4.61
Cells + cytochalasin B	0.243 ± 0.057	11.8 ± 7.20
Untreated cells	0.184 ± 0.047	2.13 ± 1.17
Cells + nocodazole	0.127 ± 0.020	2.29 ± 0.96

The results are presented as mean values ± SD. E_C and E_N symbolize Young's modulus for cortical and nuclear cells, respectively.

whole lens or its cross-section. The obtained results show that the lens nucleus is stiffer than cortex for the aged lens. Pau and Kranz measured the force required to penetrate human crystalline lenses with a large conical probe.[41] For examined lenses aged 20–84 years, a higher force was required to achieve axial lens penetration of the nucleus, compared to the cortex. The more recent studies on stiffness by Heys et al.[8] and Weeber et al.[10] were performed using dynamic mechanical analysis with small custom-built probes to evaluate stiffness at different locations on a lens cross-section. Although Heys et al. used a quasi-static penetration technique[8] and Weeber et al. used an oscillating probe,[10] the conclusions of the two studies were qualitatively similar. Both groups found that the stiffness of the adult nucleus was higher than the stiffness of the cortex. Heys et al. reported that in lenses over the age of 50, the lens nucleus typically was an order of magnitude stiffer than the cortex.[8] The mean elastic modulus value for the nucleus was 52.2 ± 14.7 kPa and 6.12 ± 2.13 kPa for the cortex in lenses older than 60 years. The results of Weeber et al. showed that at old age (70 years) the stiffness of the nucleus was 24 times higher than the stiffness of the cortex.[10] Hollman et al. used bubble-based acoustic radiation force to derive elastic properties in different regions of the human lens tissue.[42] For old-age lenses (63–70 years), Young's modulus ranged from 10.6 kPa in the center to 1.4 kPa on the periphery. Our results obtained from the measurements on isolated lens cells, that is at single cell level, are in quantitative agreement with the lens stiffness data obtained on whole lenses, that is at tissue level. It has been shown that cell stiffness varies with temperature changes.[43,44] However, given the observed maintenance of the shape of isolated fiber lens cells at room temperature, it is unlikely that the absolute stiffness would change importantly at physiological temperatures, and we expect that the relative stiffness between cortical and nuclear cells will be preserved.

It is remarkable that, unlike other types of tissues where isolated or detached cells change their shape and/or mechanical stability, isolated lens fiber cells appear to maintain their shape and elastic properties, with preserved stiffness differences between cortical and nuclear cells similar to that observed in lens tissue. These results suggest that the mechanical stability of lens fiber cells probably is not due to the common cytoskeletal filaments and an integral tension between them supported by cell-cell and cell-extracellular matrix junctions found in other tissues, but due to totally different structural elements.[45] Indeed, the addition of cytoskeleton disrupting drugs (cytochalasin B or nocodazole) did not have a significant effect on the elasticity of cortical and nuclear lens cells. These data indicate that usual cytoskeleton elements, actin and microtubules, play minor roles in lens elasticity. However, another important contributor to the lens stiffness is the intermediate filament network. A recent work on mice knocked-out of lens-specific intermediate filaments, beaded filaments, showed that the eye lens was more compliant than that of wild type mice.[46] Certainly, the absence of biochemical activity in differentiated lens fiber cells is one of the reasons for the preservation of the mechanical properties after cell removal from the tissue ensemble. We hypothesize that tightly packed crystallin proteins inside the cell have major influence on lens fiber cell stiffness and shape maintenance. A link between the α crystallin content of the human lens and its flexibility recently has been suggested.[9] It was shown that the overall decrease in soluble protein content and α crystallin with age parallels the increase in lens stiffness up to age 50. Of particular note, after 50 when all of the α crystallin has been incorporated into high molecular weight aggregates or insoluble proteins, there is an even more dramatic increase in lens stiffness.[9] Friedrich and Truscott suggested that binding of proteins to fiber cell membranes may be involved in lens stiffening.[47] The authors characterized age-related changes to proteins in the center of the human lens, and found that major changes to the lens crystallins of the nucleus take place between age 40 and 50, after the loss of free soluble α crystallin. Thus, both crystallins and beaded filaments appear to be important proteins for the mechanical stability of lens cells and should be investigated further.

In conclusion, our study indicates the capabilities of the AFM as a tool for mechanical characterization with high accuracy and at the single cell level. Doubtlessly, although the results may apply only to ovine lenses, the technique can be adapted to analyze effects of aging and pathology on lens cell mechanics. We believe that the AFM can have a significant role in ophthalmologic research providing its high-resolution imaging,[39,48–50] and cell mechanics analysis capacities. Further studies using the applied approach and targeting lens-specific intermediate filaments and/or the organization of crystallin proteins within the cell would provide deeper insights into the mechanisms of eye lens mechanics.

References

1. Donaldson P, Kistler J, Mathias RT. Molecular solutions to mammalian lens transparency. *News Physiol Sci*. 2001;16:118–123.
2. Dahm R. Dying to see. *Sci Amer*. 2004;83–89.
3. Bassnett S. On the mechanism of organelle degradation in the vertebrate lens. *Exp Eye Res*. 2009;88:133–139.
4. Andley UP. Crystallins in the eye: function and pathology. *Prog Retin Eye Res*. 2007;25:78–98.
5. Kuszak JR, Brown HG. Embryology and anatomy of the lens (Chapter 5). In: Albert DM, Jakobiec FA, eds. *Principles and Practice of Ophthalmology*. Philadelphia: W.B. Saunders Co. 1994;82–96.
6. Helmholtz H. Ueber die Accommodation des Auges. *Albrecht von Graefes Arch Ophthalmol*. 1855;1:1–74.
7. Starodubtseva MN. Mechanical properties of cells and aging. *Ageing Res Rev*. 2011;10:16–25.
8. Heys KR, Cram SL, Truscott RJW. Massive increase in the stiffness of the human lens nucleus with age: the basis for presbyopia? *Mol Vis*. 2004;10:956–963.
9. Heys KR, Friedrich MG, Truscott RJW. Presbyopia and heat: changes associated with aging of the human lens suggest a functional role for the small heat shock protein, α-crystallin, in maintaining lens flexibility. *Aging Cell*. 2007;6:807–815.
10. Weeber HA, Eckert G, Pechhold W, van der Heijde RGL. Stiffness gradient in the crystalline lens. *Graefe's Arch Clin Exp Ophthalmol*. 2007;245:1357–1366.
11. Kirmizis D, Logothetidis S. Atomic force microscopy probing in the measurement of cell mechanics. *Int J Nanomedicine*. 2010;5:137–145.
12. Binnig G, Quate CF, Gerber C. Atomic Force Microscope. *Phys Rev Lett*. 1986;56:930–934.
13. Casuso I, Rico F, Scheuring S. Biological AFM: where we come from – where we are – where we may go. *J Mol Recognit*. 2011;24:406–413.
14. Parot P, Dufréne YF, Hinterdorfer P, et al. Past, present and future of atomic force microscopy in life sciences and medicine. *J Mol Recognit*. 2007;20:418–431.
15. Radmacher M. Measuring the elastic properties of living cells by the atomic force microscopy. *Methods Cell Biol*. 2002;68:67–90.
16. Lehenkari PP, Charras GT, Nesbitt SA, Horton MA. New technologies in scanning probe microscopy for studying molecular interactions in cells. *Expert Rev Mol Med*. 2000;2:1–19.

17. Radmacher M, Fritz M, Kacher CM, Cleveland JP, Hansma PK. Measuring the viscoelastic properties of human platelets with the atomic force microscope. *Biophys J*. 1996;70:556–567.
18. Swaminathan I, Woodworth CD, Gaikwad RM, Kievsky YY, Sokolov I. Towards nonspecific detection of malignant cervical cells with fluorescent silica beads. *Small*. 2009;5:2277–2284.
19. Cross SE, Jin Y-S, Rao J, Gimzewski JK. Nanomechanical analysis of cells from cancer patients. *Nat Nanotech*. 2007;2: 780–783.
20. Sokolov I. Atomic force microscopy in cancer cell research. In: Nalwa HS, Webster T, eds. *Cancer Nanotechnology – Nanomaterials for Cancer Ciagnosis and Therapy*. Valencia, CA: American Scientific Publishers; 2006;43–59.
21. Dulińska I, Targosz M, Strojny W, et al. Stiffness of normal and pathological erythrocytes studied by means of atomic force microscopy. *J Biochem Biophys Methods*. 2006;66:1–11.
22. Lekka M, Laidler P, Ignacak J, et al. The effect of chitosan on stiffness and glycolytic activity of human bladder cells. *Biochim Biophys Acta*. 2001;1540:127–136.
23. Lekka M, Laidler P, Gil D, Lekki J, Stachura Z, Hrynkiewicz AZ. Elasticity of normal and cancerous human bladder cells studied by scanning force microscopy. *Eur Biophys J*. 1999; 28:312–316.
24. Radmacher M. Studying the mechanics of cellular processes by atomic force microscopy. *Methods Cell Biol*. 2007;83:347–372.
25. Ziebarth NM, Wojcikiewicz EP, Manns F, Moy VT, Parel J-M. Atomic Force Microscopy measurements of lens elasticity in monkey eyes. *Mol Vis*. 2007;13:504–510.
26. Ziebarth NM, Arrieta E, Feuer WJ, Moy VT, Manns F, Parel J-M. Primate lens capsule elasticity assessed using Atomic Force Microscopy. *Exp Eye Res*. 2011;92:490–494.
27. Last JA, Russell P, Nealey PF, Murphy CJ. The applications of atomic force microscopy to vision science. *Invest Ophthalmol Vis Sci*. 2010;51:6083–6094.
28. Garland DL, Duglas-Tabor Y, Jimenez-Asensio J, Datiles MB, Magno B. The nucleus of the human lens: demonstration of a highly characteristic protein pattern by two-dimensional electrophoresis and introduction of a new method of lens dissection. *Exp Eye Res*. 1996;62:285–291.
29. Hutter JL, Bechhoefer J. Calibration of atomic-force microscope tips. *Rev Sci Instrum*. 1993;64:1868–1873.
30. Pittenger B, Erina N, Su C. Quantitative mechanical property mapping at the nanoscale with PeakForce QNM. *Veeco Application Note*. 2010;AN128.
31. Rico F, Su C, Scheuring S. Mechanical mapping of single proteins at submolecular resolution. *Nano Lett*. 2011;11: 3983–3986.
32. Ludwig T, Kirmse R, Poole K, Schwarz US. Probing cellular microenvironments and tissue remodeling by atomic force microscopy. *Eur J Physiol*. 2008;456:29–49.
33. Hertz H. "Über die Berührung fester elastischer Körper (On Contact Between Elastic Bodies)." *J Reine Angew Math*. 1881; 92,156–171. [English transl. Hertz H. On the contact of elastic solids. In: Jones DE, Schott GA, eds. *Miscellaneous Papers by H. Hertz*. London: Macmillan; 1896:146–162.].
34. Rico F, Roca-Cusachs P, Gavara N, Farré R, Rotger M, Navajas D. Probing mechanical properties of living cells by atomic force microscopy with blunted pyramidal cantilever tips. *Phys Rev E Stat Nonlin Soft Matter Phys*. 2005;72:021914.
35. Kistler J, Gilbert K, Brooks HV, Jolly RD, Hopcroft DH, Bullivant S. Membrane interlocking domains in the lens. *Invest Ophthalmol Vis Sci*. 1986;27:1527–1534.
36. Kuznetsova TG, Starodubtseva MN, Yegorenkov NI, Chizhik SA, Zhdanov RI. Atomic force microscopy probing of cell elasticity. *Micron*. 2007;38:824–833.
37. Kuszak JR, Zoltoski RK, Sivertson C. Fibre cell organization in crystalline lenses. *Exp Eye Res*. 2004;78:673–687.
38. Augusteyn RC. Growth of the lens: in vitro observations. *Clin Exp Optom*. 2008;91:226–239.
39. Buzhynskyy N, Hite RK, Walz T, Scheuring S. The supramolecular architecture of junctional microdomains in native lens membranes. *EMBO Reports*. 2007;8:51–55.
40. Augusteyn RC, Stevens A. Macromolecular structure of the eye lens. *Prog Polym Sci*. 1998;23:375–413.
41. Pau H, Kranz J. The increasing sclerosis of the human lens with age and its relevance to accommodation and presbyopia. *Graefe's Arch Clin Exp Ophthalmol*. 1991;299:294–296.
42. Hollman KW, O'Donnell M, Erpelding TN. Mapping elasticity in human lenses using bubble-based acoustic radiation force. *Exp Eye Res*. 2007;85:890–893.
43. Rico F, Chu C, Abdulreda MH, Qin Y, Moy VT. Temperature modulation of integrin-mediated cell adhesion. *Biophys J*. 2010;99:1387–1396.
44. Sunyer R, Trepat X, Fredberg JJ, Farré R, Navajas D. The temperature dependance of cell mechanics measured by atomic force microscopy. *Phys Biol*. 2009;6:025009.
45. Ingber DE. Cellular mechanotransduction: putting all the pieces together again. *FASEB J*. 2006;20:811–827.
46. Fudge DS, McCuaig JV, Van Stralen S, et al. Intermediate filaments regulate tissue size and stiffness in the murine lens. *Invest Ophthalmol Vis Sci*. 2011;52:3860–3867.
47. Friedrich MG, Truscott RJ. Membrane association of proteins in the aging human lens: profound changes take place in the fifth decade of life. *Invest Ophthalmol Vis Sci*. 2009;50:4786–4793.
48. Buzhynskyy N, Girmens J-F, Faigle W, Scheuring S. Human cataract lens membrane at subnanometer resolution. *J Mol Biol*. 2007;374:162–169.
49. Mangenot S, Buzhynskyy N, Girmens J-F, Scheuring S. Malformation of junctional microdomains in cataract lens membranes from a type II diabetes patient. *Pflugers Arch - Eur J Physiol*. 2009;457:1265–1274.
50. Buzhynskyy N, Salesse C, Scheuring S. Rhodopsin is spatially heterogeneously distributed in rod outer segment disk membranes. *J Mol Recognit*. 2011;24:483–489.